ENDOR and pulsed ESR study of proton glass behavior in the mixed crystal (betaine phosphate)$_{0.15}$(betaine phosphite)$_{0.85}$

H. Bauch, G. Völkel, R. Böttcher, A. Pöppl, and H. Schäfer
Universität Leipzig, Fakultät für Physik und Geowissenschaften, D-04103 Leipzig, Germany

J. Banys
University of Vilnius, Faculty of Physics, 2054 Vilnius, Lithuania

A. Klöpperpieper
Universität des Saarlandes, Fachbereich Physik, D-66123 Saarbrücken, Germany

(Received 11 April 1996)

The proton ENDOR spectra of $BP_{0.15}BPI_{0.85}$ taken between 90 and 290 K allow a direct determination of the local polarization distribution $W(p)$ of the protons in the hydrogen bonds linking the phosphate and phosphite groups to chains. The temperature dependence of the Edwards-Anderson glass order parameter can be described by a random-field dominated proton glass behavior in $BP_{0.15}BPI_{0.85}$ with a glass temperature of $T_G=30$ K and a random-field induced freezing temperature of $T_f=(95\pm5)$ K. The experimental results do not permit one to discriminate between three-dimensional (3D) or quasi-one-dimensional interactions of the hydrogen bonds. The experimentally determined polarization distribution function $W(p)$ can be described to a certain extent within the 3D random-bond random-field model if a long-range order of the protons is introduced by a non-zero mean $\tilde{J}_0/k_B=160$ K of the random-bond interaction. Additionally, the local field variance $\tilde{\Delta}$ has to be taken as a temperature-dependent parameter with a minimal value at the resulting phase transition at 144 K. However, even at lowest temperatures the maxima of the order parameter distribution function $W(p)$ appear at values of the local proton polarization distinctly smaller than one. This is not describable within the above models. We conclude that proton tunneling is of importance in betaine phosphite-phosphate proton glasses. [S0163-1829(96)05938-3]

I. INTRODUCTION

Betaine phosphite (BPI) $(CH_3)_3NCH_2COOH_3PO_3$ and betaine phosphate (BP) $(CH_3)_3NCH_2COOH_3PO_4$ belong to the well-known family of betaine additive compounds[1–4] which shows an impressive variety of ordered phases. Both compounds, BPI and BP, undergo a phase transition from a paraelectric high-temperature phase with space group $P2_1/m$ to an antiferrodistortive phase with space group $P2_1/c$ at 355 K (BPI) and 365 K (BP), respectively. BPI experiences a second transition into a ferroelectric ordered low-temperature phase with space group $P2_1$ at 220 K. BP shows two further structural transitions at 86 K into a ferroelectric intermediate phase of $P2_1$ symmetry,[5] and at 81 K into an antiferroelectric low-temperature phase with doubling of the unit cell along the crystallographic a direction. The structure of both compounds[6,7] is very similar. The inorganic tetrahedral PO_4 or HPO_3 groups are linked by hydrogen bonds forming zig-zag chains along the monoclinic b axis (Fig. 1). The betaine molecules are arranged almost perpendicular to this chains along the a direction and linked by one (BPI) or two (BP) hydrogen bonds to the inorganic group. The temperature dependence of the dielectric permittivity of both compounds shows evidence for a quasi-one-dimensional behavior as the coupling between the electric dipolar units along the chains is much stronger than perpendicular to it.[7,8]

Deuteration of the hydrogen bonds leads to an increase of the transition temperature into the low-temperature phases of BP and BPI by about 70 K.[9,10] This gives strong evidence that the hydrogen bonds play an important role in the ferroelectric and antiferroelectric transition. In recent papers[11–15] we studied the phase transitions and the proton order in the hydrogen bonds in BPI by means of electron spin resonance (ESR), electron nuclear double resonance (ENDOR) and

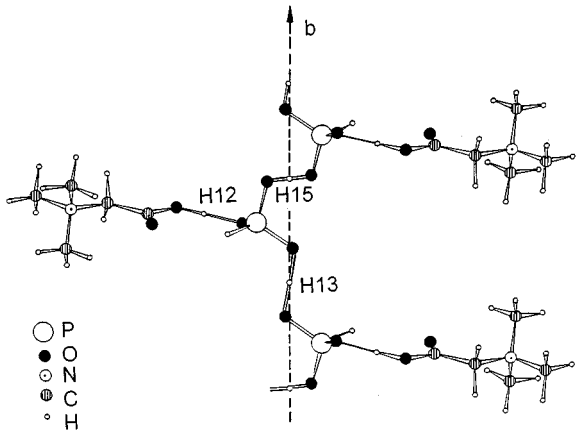

FIG. 1. Schematic drawing of the structure of betaine phosphite showing the chains of HPO_3 groups linked by hydrogen bonds with the protons $H13$ and $H15$. The betaine molecules are bound to the HPO_3 groups by one hydrogen bond with the proton $H12$. In the mixed crystal, HPO_3 is partially substituted by PO_4 to which the betaine is bound by two hydrogen bonds. Projection on the crystallographic ab plane with the atomic coordinates taken from Ref. 7.

electron spin echo envelope modulation (ESEEM) techniques. We showed that the ferroelectric transition in BPI is closely related to the ordering of the protons in the two hydrogen bonds linking the HPO_3 groups to chains along the crystallographic b axis. Dielectric measurements on BPI (Ref. 16) revealed that the ferroelectric transition of order-disorder type is caused by a relaxational soft mode related to the proton motion. The ordering processes in BP and BPI show some certain similarities with that of representatives of the well-known KH_2PO_4 (KDP) family[17] in so far as also the ordering of the protons in the double minimum potential of hydrogen bonds linking the PO_4 or HPO_3 groups appears to be the most striking structural order mechanism. However, whereas in the KDP family the hydrogen bridges form a three-dimensional network, the hydrogen bonds in the betaine compounds are arranged in quasi-one-dimensional chains which results in a peculiar ordering behavior.

The two almost isostructural compounds BP and BPI form solid solutions at any concentration. Similar as in the KDP family, mixed crystals of antiferroelectric betaine phosphate and ferroelectric betaine phosphite BP_xBPI_{1-x} show phase transitions to long-range ordered or to glassy states in dependence on the ratio x of both compounds.[18–22] The phase diagram of BP_xBPI_{1-x} can be divided into three regions: a first one with $x>0.7$ where a transition into an antiferroelectric ordered state appears, a second one with $0.7>x>0.1$ in which glassy behavior is observed at low temperatures, and a third region with a ferroelectric ordered low temperature phase for $x<0.1$. Dielectric measurements revealed proton glass behavior for $x=0.15$, 0.20, 0.40, 0.50, and 0.60.[18,21–23] Recently, the static freezing transition at finite temperature was found in a deuterated mixed crystal with $x=0.40$.[24]

The glassy state in hydrogen bonded mixed crystals consisting of a ferroelectric and an antiferroelectric component is considered to be a consequence of frustrating interactions of the electric dipoles formed by the O-H...O bonds. To decide whether the glassy transition is driven by randomly frustrated competing interactions[7–9] or governed by strong random fields, it is necessary to know the temperature dependence of the Edwards-Anderson glass order parameter q.[25–29]

Recently, we showed by ESR and ENDOR studies[11–15] that γ irradiation of BPI single crystals produces stable PO_3^{2-} centers (electron spin $S=\frac{1}{2}$) which are appropriate probes to investigate the local polarization of the protons in the hydrogen bridges linking the phosphite groups to chains along the b axis. We showed that a linear relation exists between the ENDOR line shift and the spontaneous polarization at various temperatures. Therefore, the investigation of the temperature dependence of the ^1H electron nuclear double resonance (ENDOR) spectra in γ irradiated $BP_{0.15}BPI_{0.85}$ should allow one to measure the local polarization distribution of the protons in this mixed compound and to draw conclusions on the ordering behavior. As recently shown (Ref. 30), ^1H ENDOR spectra analyzed with the Tikhonov regularization method provide a direct experimental access to the local polarization distribution function $W(p)$ which is directly related to the Edwards-Anderson parameter q.

In comparison to NMR spectroscopy the ENDOR technique has the advantage that because of the hyperfine interaction of protons with the paramagnetic PO_3^{2-} probe one can select the protons of interest in the hydrogen bonds linking the phosphorous groups to chains along the b axis from all the other protons present in the compound. The hyperfine coupling changes very sensitively with the variation of the proton distance from the PO_3^{2-} center. And last but not least, this technique is applicable also to deuterated or partially deuterated samples so that a direct comparison of the local proton and deuteron order becomes practicable even in the same sample. This is of special interest with respect to the still open problem of proton tunneling.[31,32] Another problem is related with the proton dynamics. It is important to know if the thermal proton motion within the hydrogen bond is slow or fast with respect to the time scale of the experiment. Such a determination can be made by means of a two-dimensional electron spin echo envelope modulation (2D ESEEM) technique using the HYSCORE (hyperfine sublevel correlation spectroscopy) sequence.[33] This experiment permits one to separate the homogeneous from the inhomogeneous part of the broadening of an ENDOR line.[34] The homogeneous line broadening is a sensitive measure of the slowing down of the proton dynamics. In this paper the proton order in the $BP_{0.15}BPI_{0.85}$ mixed crystal is studied by ENDOR, HYSCORE and electron spin relaxation time measurements.

II. EXPERIMENTAL

$BP_{0.15}BPI_{0.85}$ single crystals were grown by controlled evaporation from aqueous solution containing betaine with 15% of H_3PO_3 and 85% H_3PO_4. For ENDOR investigations the crystals were γ irradiated with a dose of about 2 Mrad to form the paramagnetic PO_3^{2-} probe. The ESR, ENDOR, and ESEEM experiments have been carried out with a Bruker ESP 380 E FT/CW ESR spectrometer working in x band. Temperature variations in the range from 77 to 290 K were done with a liquid nitrogen flow cryostat whereas measurements below 77 K were performed using an Oxford CF 935 cryostat. All ENDOR experiments were performed by saturation of the high field ESR line of the PO_3^{2-} centers. For the ESEEM experiments pulse lengths of 12 ns for $\pi/2$ pulses and 24 ns for π pulses were used. In the 2D spectra 256 points were sampled with 126 ns increment in both time domains t_1 and t_2. A four-step phase cycle was used to avoid interference with unwanted two and three pulse echoes. The echo decay has been eliminated by a fourth-order polynominal base line correction of the experimental data set in both time domains. No apodization functions were used to avoid additional line shape distortions. Before 2D Fourier transformation (FT) the data set was zero filled to 1 kilo-byte in both time domains. After 2D Fourier transformation the power spectra were calculated and presented as contour plots. The spin-lattice relaxation time T_1 was measured by means of the inversion recovery method using π-T-$\pi/2$-τ-π-τ-echo sequence or by signal saturation of the primary echo with changing the repetition rate $\pi/2$-τ-π-τ-echo-T-$\pi/2$-τ-π-τ-echo-$T\cdots$. During the experiments τ was kept constant whereas T was changed. The pulse widths used were the same as in the ESEEM experiment.

III. THEORETICAL

ENDOR line shape

In proton glasses the local polarization p of the O-H...O bonds is distributed according to a probability function $W(p)$. The second moment of this probability distribution $W(p)$ is the Edwards-Anderson glass order parameter[28]

$$q=\int_{-1}^{+1} dp\ W(p)p^2. \tag{1}$$

A simple relation between the probability distribution $W(p)$ and the ENDOR line shape exists when the ENDOR frequency ω of a single proton in such a bond depends linearly on the local polarization:

$$\omega=\omega_0+\omega_1 p, \tag{2}$$

where ω_1 is the ENDOR line shift at $p=\pm 1$ with respect to the ENDOR line position ω_0 at $p=0$.

Considering a fluctuating proton in a hydrogen bond its individual line shape $I(\omega,p)$ can be described as that for chemical exchange in an asymmetric two site potential[28]

$$I(\omega,p)=\frac{1}{\pi}\frac{\Gamma\omega_1^2(1-p^2)}{(\omega^2-\omega_1^2)^2+\Gamma^2(\omega-\omega_1 p)^2}, \tag{3}$$

where Γ is a phenomenological parameter called the relaxation rate. For a Markov process the rate is given by

$$\Gamma=\frac{1}{\tau_+}+\frac{1}{\tau_-} \tag{4}$$

with $\tau_+=\tau_-\exp(-2\Delta E/k_BT)$. The quantities τ_+ and τ_- are the average dwell times in the left or right minimum of the asymmetric local double minimum potential with bias energies $\pm\Delta E$. The local static polarization of the proton in a hydrogen bond can be written as

$$p=(\tau_--\tau_+)/(\tau_-+\tau_+)=\tanh(\Delta E/k_BT). \tag{5}$$

The ^{1}H ENDOR line shape of the proton in the proton glass is then given by[28]

$$I(\omega)=\int_{-1}^{+1} W(p)I(\omega,p)dp. \tag{6a}$$

Consequently, the probability distribution $W(p)$ of the local order parameter p can be obtained directly by analyzing the ENDOR line shape. We have to distinguish two cases:

In the fast motion limit $\Gamma\gg 2\omega_1$ the line shape function $I(\omega,p)$ behaves nearly as a Dirac δ function $\delta(\omega-\omega_1 p)$ and, therefore, the line shape of the ^{1}H ENDOR spectrum is simply

$$I(\omega)=\frac{1}{\omega_1}W(\omega/\omega_1). \tag{6b}$$

In the intermediate ($\Gamma\sim 2\omega_1$) and slow motion regime ($\Gamma\ll 2\omega_1$) additional broadenings and line shifts appear making the relationship between ENDOR line shape and order parameter distribution function $W(p)$ more complicated. In order to extract $W(p)$ from the ENDOR line shape, the integral in Eq. (6a) must be solved numerically. As shown in a previous paper,[30] the Tikhonov regularization method can successfully be used to determine the local polarization distribution $W(p)$ from magnetic resonance line shapes. The great advantage of this method is that one does not need model assumption about $W(p)$, one uses all the information given in the experimental data, and there are no restrictions necessary for the relaxation rate Γ.

3D RBRF Ising Model

In the next section we will make comparisons with two models, the three-dimensional random-bond random-field (3D RBRF) Ising model of Pirc *et al.*[28] and the quasi-one-dimensional random-bond random field (1D RBRF) model of Oresic and Pirc.[35] Therefore, we shall briefly repeat the results for these models.

In Ref. 28 the authors presented a dynamic theory of the deuteron NMR line shape in deuteron glasses based on the infinitely ranged random-bond Ising model with the addition of quenched local random fields (3D RBRF Ising model). The pseudo-spin glass can be described by the model Hamiltonian

$$H=-\tfrac{1}{2}\sum_{i,j} J_{ij}\sigma_i\sigma_j-\sum_i f_i\sigma_i, \tag{7a}$$

where the pseudospin $\sigma_i=\pm 1$ refers to the left-right position of a proton (deuteron) in the ith hydrogen bond. The random interactions J_{ij} distributed according to a Gaussian probability density are assumed to be infinitely ranged with a mean value

$$J_0=\widetilde{J}_0/N=\langle J_{ij}\rangle \tag{7b}$$

and a variance

$$J=\widetilde{J}/N^{1/2}=\mathrm{var}\{J_{ij}\}. \tag{7c}$$

The random electric fields f_i due to substitutional disorder are also Gaussian distributed with a variance

$$\sqrt{\Delta}=\mathrm{var}\{f_i\} \tag{7d}$$

and a zero mean value. For $|\widetilde{J}_0|\gtrsim\widetilde{J}$ a transition into a long-ranged ordered ferroelectric ($\widetilde{J}_0>0$) or antiferroelectric ($\widetilde{J}_0<0$) phase takes place[27] whereas for $|\widetilde{J}_0|<\widetilde{J}$ a low-temperature pseudo-spin-glass phase appears. The latter phase is characterized by a zero long-range order parameter $\overline{p}=(1/N)\Sigma_i\langle\sigma_i\rangle$ but a nonzero Edwards-Anderson glass order parameter $q=(1/N)\Sigma_i\langle\sigma_i\rangle^2$. Here N is the number of pseudospins of the system. The local pseudospin polarization

$$p=\tanh[h(z)/k_BT] \tag{8}$$

is determined by the Gaussian random field

$$h(z)=\widetilde{J}(q+\widetilde{\Delta})^{1/2}z+\widetilde{J}_0\overline{p} \tag{9}$$

at the position of the quasispin where z is a Gaussian random number and $\widetilde{\Delta}=\Delta/\widetilde{J}^2$. The order parameters are given by the two coupled self-consistent equations

$$\overline{p}=\int_{-\infty}^{+\infty}\frac{dz}{\sqrt{2\pi}}e^{-z^2/2}\tanh[h(z)/k_BT] \tag{10}$$

and

$$q=\int_{-\infty}^{+\infty}\frac{dz}{\sqrt{2\pi}}\,e^{-z^2/2}\tanh^2[h(z)/k_BT]. \tag{11}$$

Introducing the local polarization p from Eq. (8) as a new integration variable one can rewrite Eq. (10) as[27,28]

$$\overline{p}=\int_{-\infty}^{+\infty}dp\;W(p)p, \tag{12}$$

where

$$W(p)=\frac{1}{(\tilde{J}/k_BT)[2\pi(q+\tilde{\Delta})]^{1/2}}\frac{1}{1-p^2}\times\exp\left(-\frac{[\arctan\,h(p)-J_0\overline{p}/k_BT]^2}{2(\tilde{J}/k_BT)^2(q+\tilde{\Delta})}\right) \tag{13}$$

represents the static equilibrium probability distribution of the local polarization p which was already used in Eq. (1). The glass temperature T_G and the freezing temperature T_f are related to the variances $\tilde{J}$ and Δ of the Gaussian distributed random bonds J_{ij} and random fields f_i, respectively, in the following manner:[29]

$$\tilde{J}=k_BT_G \quad \text{for } \Delta=0, \tag{14}$$

and

$$\sqrt{\Delta}=k_BT_f. \tag{15}$$

For $\Delta\neq0$ the Edwards-Anderson glass order parameter according to Eq. (11) is different from zero at temperatures already far above the nominal glass temperature T_G.

1D RBRF Ising Model

In the model of a quasi-one-dimensional spin glass,[35] a system of linear chains of Ising spins is considered. It is supposed that a short-range nearest-neighbor ferroelectric interaction of strength K acts along the chains, whereas an infinite-range random interaction of a Sherrington-Kirkpatrick type with the variance $\tilde{J}$ is effective between different chains. The model includes also local Gaussian random fields with variance Δ. The model Hamiltonian for such a system of N Ising spins $\sigma_i=\pm1$ arranged in a set of linear chains is formally written as

$$H=-\sum_{(ij)}K_{ij}\sigma_i\sigma_j-\sum_{(ij)}J_{ij}\sigma_i\sigma_j-\sum_i f_i\sigma_i, \tag{16}$$

where $K_{ij}=K>0$ if i and j are nearest neighbors within a chain but $K_{ij}=0$ otherwise. The quenched random interactions J_{ij} and the local random fields f_i are Gaussian distributed with zero mean values. Using the replica formalism, recursion relations for the local polarization $p_i=\langle\sigma_i\rangle_{1D}$ were given [Eq. (27) in Ref. 35] which allow one to calculate numerically the glass order parameter [Eq. (36) in Ref. 35]

$$q=\frac{1}{N}\sum_{i=1}^{N}\langle\sigma_i\rangle_{1D}^2. \tag{17}$$

The recursion relations contain only the ferroelectric interaction K, the local fields $h(z)$ and the temperature T. After the local polarizations p_i of all the N spins were numerically calculated, we determined the probability distribution $W(p)$ of the local order parameter by counting off the spins which have their local polarization within an interval between p and $p+\Delta p$.

IV. EXPERIMENTAL RESULTS

ENDOR and ESEEM measurements

The ESR spectra of γ irradiated $BP_{0.15}BPI_{0.85}$ at 290 K show a doublet structure with a hyperfine splitting of more than 50 mT typical for a PO_3^{2-} radical at a phosphite group of the mixed crystal. This doublet splitting is due to the hyperfine interaction of the unpaired electron localized in one sp^3 phosphorus orbital with the ^{31}P nuclear spin $I=\frac{1}{2}$. The observed two doublets for an arbitrary direction of the external magnetic field with respect to the crystallographic axes indicate two magnetically nonequivalent positions of the PO_3^{2-} center according to the expected space group $P2_1/c$ in the antiferrodistortive phase. In contradiction to the pure BPI single crystals[15] no further splitting of the ESR lines was observed in the mixed crystal $BP_{0.15}BPI_{0.85}$ in the temperature range from 290 down to 10 K but a remarkable increase in line width occurs to lower temperatures.

Saturating the high field ESR line at different directions of the external magnetic field with respect to the crystallographic axes of the $BP_{0.15}BPI_{0.85}$ samples, the angular dependencies of the ^1H ENDOR spectra were investigated. In contrast to the ^1H ENDOR spectra of the pure BPI crystal[11,12] which show sharp lines, we observed strongly broadened

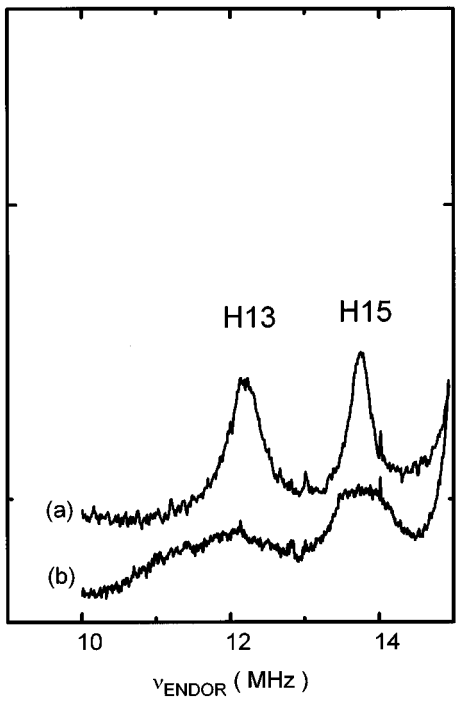

FIG. 2. Low frequency part of the ^1H ENDOR spectra of the PO_3^{2-} center in γ irradiated (a) BPI and (b) $BP_{0.15}BPI_{0.85}$ taken at room temperature with the magnetic field $B\|c$.

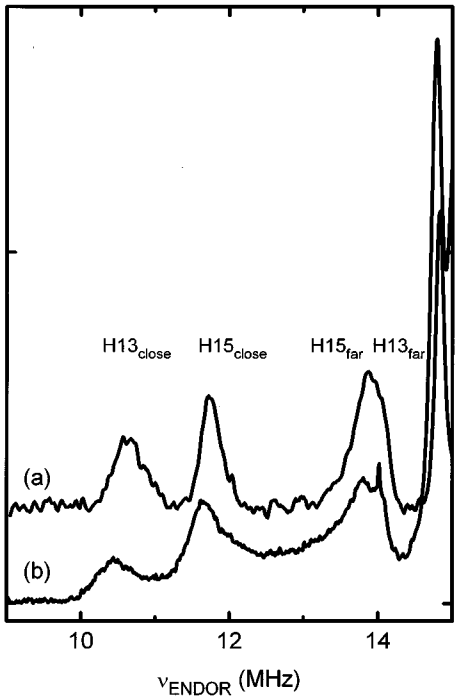

FIG. 3. Low frequency part of the ^{1}H ENDOR spectra of the PO_3^{2-} center in γ-irradiated (a) BPI and (b) $BP_{0.15}BPI_{0.85}$ taken at 100 K with the magnetic field $\underline{B} \| c$. The marks ''close'' and ''far'' correspond to the possible mean positions of the protons $H13$ and $H15$ with respect to the PO_3^{2-} center at low temperatures.

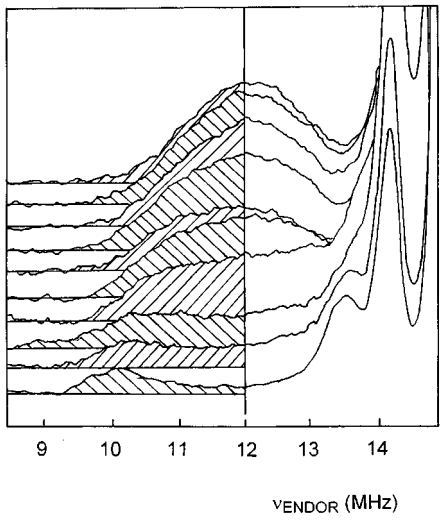

FIG. 4. Temperature dependence of the ^{1}H ENDOR line of proton $H13$ at PO_3^{2-} center in γ-irradiated $BP_{0.15}BPI_{0.85}$ taken from 290 K (upper spectrum) down to 90 K (lower spectrum) in steps of 20 K with the magnetic field $\underline{B}$ in the crystallographic ac plane forming an angle of 20° with the c direction. The hatching marks the part of the spectra which is not overlapped by other lines and, therefore, used for the calculations.

ENDOR lines in the spectra of the mixed crystals $BP_{0.15}BPI_{0.85}$ from room temperature (Fig. 2) down to 100 K (Figs. 3 and 4). We determined the hyperfine structure tensors (Table I) from the angular dependencies of the ^{1}H ENDOR lines (Fig. 5) and compared them with the results of our ENDOR investigation of the pure BPI crystal. Eigenvalues and eigenvectors of the measured hfs tensors for the line centers of the protons in $BP_{0.15}BPI_{0.85}$ are in good agreement with those for the protons $H12$, $H13$ and $H15$ in pure BPI.[11] Therefore, the ^{1}H ENDOR lines in $BP_{0.15}BPI_{0.85}$ can be assigned to the protons $H12$, $H13$, and $H15$ in the O-H...O bonds adjacent to the PO_3^{2-} centre in the mixed crystal. The temperature dependence of the ^{1}H ENDOR line shape of the protons $H13$ and $H15$ linking neighboring HPO_3/PO_4 was measured in the temperature range from 290 to 90 K. As an example, the ENDOR spectra of proton $H13$ are illustrated in Fig. 4. The line shape and line width of the ^{1}H ENDOR spectra of the proton $H12$ do not indicate any temperature dependence whereas those of protons $H13$ and $H15$ show very strong changes from room temperatures down to low temperatures. We observed a change in the line shape from a nearly Gaussian line of up to 2 MHz line width at 300 K [Figs. 2(b) and 4] to a flattened shape at intermediate temperatures and further into a double peak structure at low temperatures [Fig. 3(b)]. The angular dependencies of the ENDOR lines with the double peak structure were measured at 77 K [Fig. 5(b)]. The hfs tensors of both peak positions were determined and appeared to agree with those in BPI at 77 K (Ref. 11) indicating that the peaks correspond to the ''close'' and ''far'' positions of the protons $H13$ and $H15$. Because the ^{1}H ENDOR line shape of these protons show a double peak structure with extended parts of intensity between the peaks marking the ''close'' and ''far'' positions, either the individual hfs parameters of the protons must remarkably scatter or strong motional effects must govern the line shape. In order to distinguish between both cases, pulse ESR experiments were performed.

HYSCORE experiments indicate that the protons in the hydrogen bridges are always close to the fast-motion limit with $\Gamma \gg 2\omega_1$ at temperatures above 70 K. The distribution of the proton hyperfine couplings related to the probability distribution of the local proton order in the hydrogen bonds leads to ridge-type cross-peaks perpendicular to the frequency diagonal $\nu_1 = \nu_2$ of the 2D HYSCORE spectra[34,36] as shown in Fig. 6. The extension of the ridge-type cross peak parallel to the frequency diagonal $\nu_1 = \nu_2$ is a measure of the homogeneous line width of each of the individual cross peaks at distinct frequencies. This individual homogeneous line width should significantly increase when the proton dynamics change from the fast to the slow motion limit. Because $\omega_1/2\pi$ is of the order of 3 MHz for the direction of applied magnetic field used in Fig. 4, one would expect really strong and remarkable changes in the ENDOR spectra for decreasing temperatures. The temperature dependence of the homogeneous width in half height of the $H13$ cross peaks taken from the 2D spectra shown in Fig. 6 is given in Fig. 7. The homogeneous width increases up to 300 kHz at 120 K. An estimation of the line width using Eq. (3) with $p = 0.6$, $\omega_1/2\pi = 3$ MHz leads to a relaxation rate $\Gamma/2\pi = 40$ MHz. In this estimation, one has to take into consideration that the width plotted in Fig. 7 is overestimated because it contains an additional contribution of 0.12 MHz due to the finite length of the time window for the data set of 4.1 μs. Consequently, from this experiment we may conclude that the relaxation rate $\Gamma/2\pi$ in the investigated temperature range is higher than 40 MHz. This is in agreement with the dielectric

TABLE I. Principle values and eigenvectors of the hfs tensors for the protons $H12$, $H13$, and $H15$ in the mixed crystal $BP_{0.15}BPI_{0.85}$ at the temperatures $T=290$ and $T=77$ K. The reference frame is the rectangular coordinate system with $a^*\perp bc$ plane. The indices $p=\pm 0.7$ mean that the hfs tensors were determined for the peak positions of the ENDOR spectra corresponding to the local order parameters $p=\pm 0.7$.

	A_{iso} (MHz)	A_{aniso} (MHz)	Principal axes a^*	b	c	Error (MHz)
			$T=290$ K			
		−2.5	0.827	0.313	−0.468	
$H13$	−2.0	−6.0	0.425	0.197	0.883	±0.2
		+8.5	−0.368	0.929	−0.030	
		−2.1	0.230	−0.646	0.727	
$H15$	−2.2	−6.1	−0.488	0.570	0.661	±0.2
		+8.2	0.842	0.507	0.184	
		−2.3	−0.206	0.293	0.934	
$H12$	−0.4	−5.2	0.245	0.939	−0.240	±0.1
		+7.5	0.947	−0.180	0.266	
			$T=77$ K			
		−2.9	0.647	0.300	−0.701	
$H13_{p=+0.7}$	−5.1	−9.4	0.624	0.320	0.713	±0.3
		+12.3	−0.438	0.899	−0.020	
		−1.9	0.644	0.333	−0.689	
$H13_{p=-0.7}$	−1.2	−4.1	0.598	0.343	0.724	±0.4
		+6.0	−0.477	0.878	−0.021	
		−3.8	0.188	−0.414	0.891	
$H15_{p=+0.7}$	−4.5	−7.9	−0.588	0.678	0.440	±0.3
		+11.7	0.786	0.607	0.116	
		−3.2	0.366	−0.371	0.853	
$H15_{p=-0.7}$	−0.5	−4.4	0.721	−0.466	−0.512	±0.4
		+7.6	0.588	−0.803	0.097	
		−2.9	−0.215	0.399	−0.892	
$H12$	+0.1	−4.4	0.175	0.914	−0.367	±0.2
		+7.3	0.961	−0.077	0.266	

measurements[21] which showed that the relaxation rates are larger than 10 MHz above 50 K.

Therefore it is justified to assume that the double peak structure of the ^{1}H ENDOR lines of the protons $H13$ and $H15$ at 90 K and the large line width of a nearly Gaussian shaped line at 290 K are indications for a distribution $W(p)$ of the local proton polarization, as expected for a proton glass. The change from a Gaussian to a flattened line shape and further into a double peak structure is typical for magnetic resonance line shapes in proton and deuteron glasses.[29]

The measured ENDOR line shapes were analyzed by the Tikhonov regularization method to deduce the local polarization distribution $W(p)$.[30] This analysis shows also that the protons $H13$ and $H15$ are always close to the fast motion limit in the investigated temperature range. Figure 8 represents the resulting order parameter distribution functions $W(p)$ at different temperatures. The onset of a double peak structure of $W(p)$ for $T\leqslant 140$ K already far above the glass

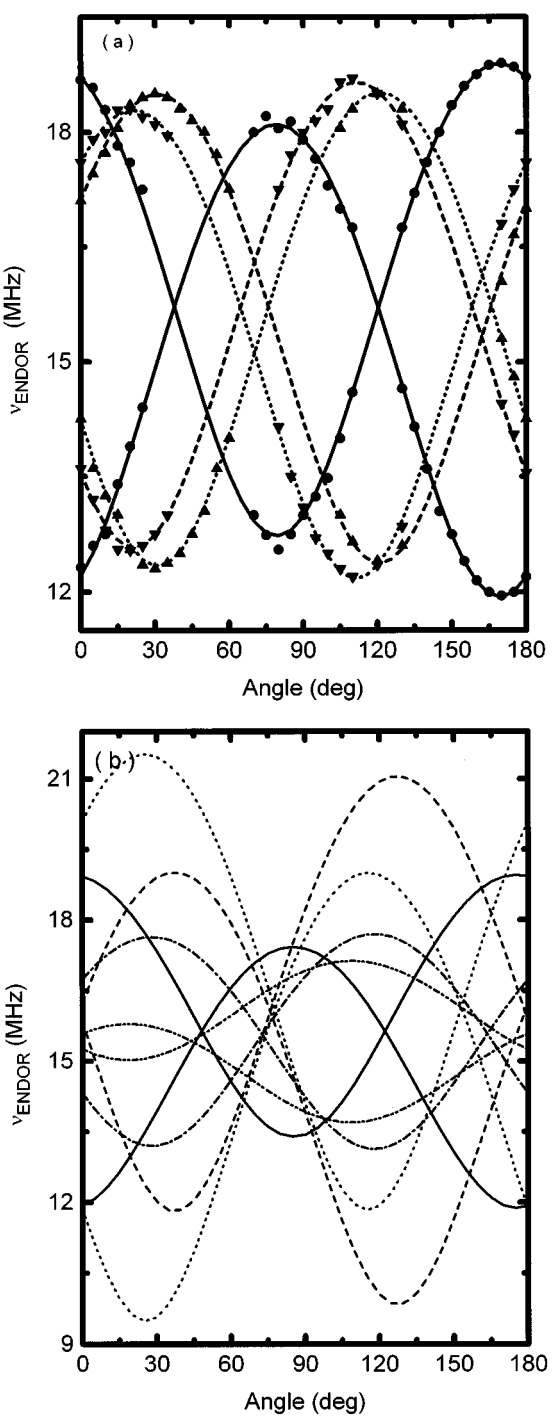

FIG. 5. Angular dependence of the ^{1}H ENDOR spectra of the PO_3^{2-} center in γ-irradiated $BP_{0.15}BPI_{0.85}$ with $\underline{B}$ rotating around the c axis at (a) $T=290$ K: (●) $H12$, (▲) $H13$, (▼) $H15$ and (b) at $T=77$ K: (—) $H12$, (---) $H13_{p=0.7}$, (−−) $H13_{p=-0.7}$, (−−−−) $H15_{p=0.7}$, (−−−) $H15_{p=-0.7}$.

temperature $T_G=30$ K known from dielectric measurements[21] is a special experimental peculiarity which has to find its explanation within the given models. The Edwards-Anderson order parameter q numerically calculated as the second moment of $W(p)$ according to Eq. (1) is shown in Fig. 9. It is evidently different from zero already far above T_G. This verifies that random fields play an important role in $BP_{0.15}BPI_{0.85}$.

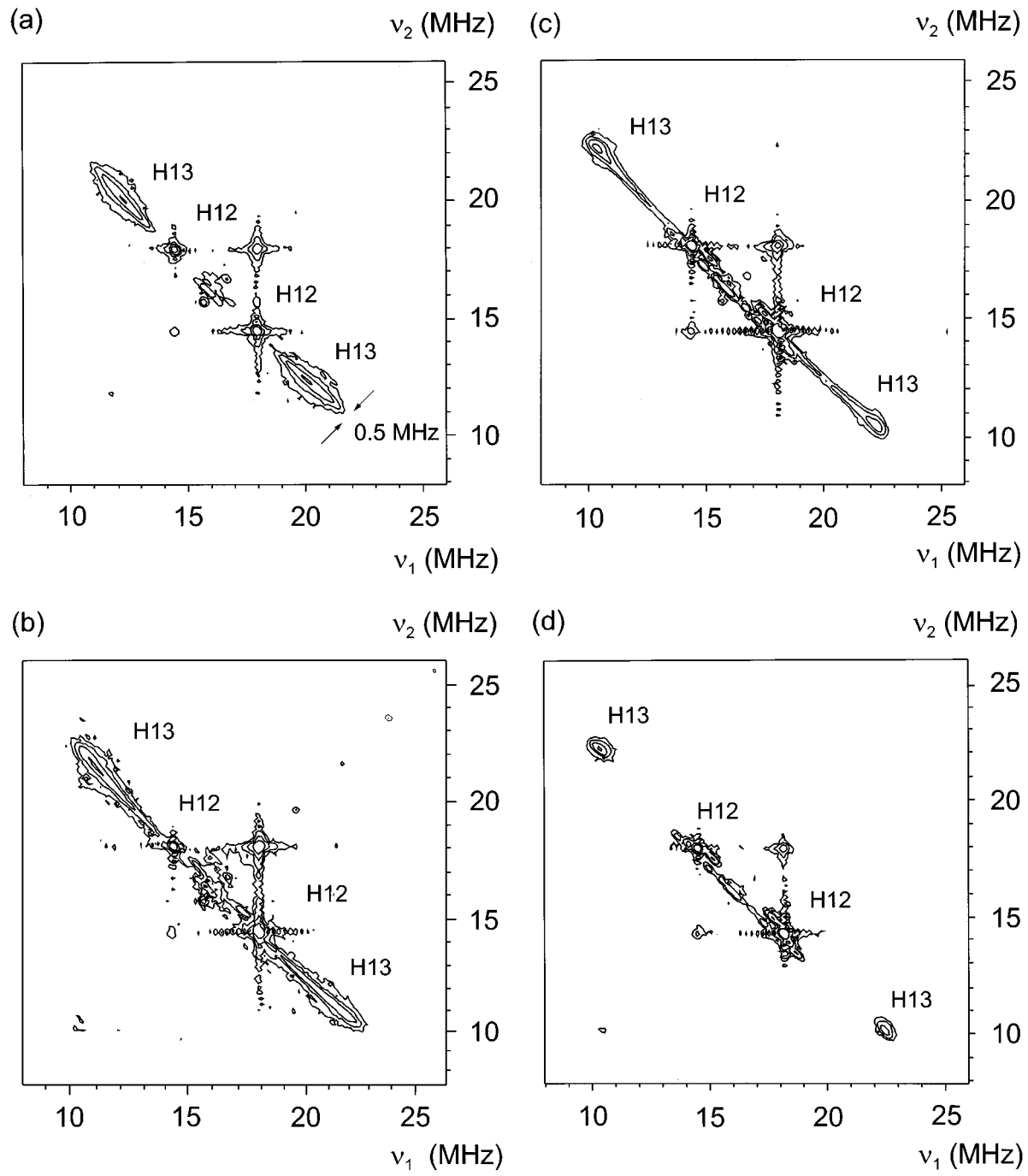

FIG. 6. 2D HYSCORE spectra of protons $H12$ and $H13$ measured at the PO_3^{2-} center in γ-irradiated $BP_{0.15}BPI_{0.85}$ at the temperatures (a) 297, (b) 140, (c) 70, and (d) 10 K. The magnetic field $\underline{B}$ is applied in the ac plane forming an angle of 35° with the c direction. Adjacent contour lines differ by a factor of 2 in intensity. The cross peaks of proton $H13$ in its ''far'' position are overlapped by those of proton $H12$. A scale bar indicating the extension of the cross peaks due to homogeneous broadening was drawn in Fig. 6(a).

One very important point in concluding from the ENDOR spectra to $W(p)$ is the normalization of the line positions with respect to the local order parameter p. This is of special importance because we will see that the probability maximum of the local order parameter never shifts up to $p=1$ not even at lowest temperatures. Within the Tikhonov regularization calculations the normalization was self-consistently done introducing ω_1 as an adjustable parameter which was numerically optimized. Otherwise, it is obviously seen by comparing the ENDOR spectra in Fig. 4 and the calculated $W(p)$ probability distribution functions given in Fig. 8 that this normalization is correct. Because we are in the fast-motion regime at all temperatures, the ENDOR lines must be decayed to zero at frequencies above or below the border line frequency $\omega^*=\omega_0\pm\omega_1$ corresponding to $p=\pm 1$. In the spectra in Fig. 4, this is the case at $\omega^*/2\pi=9.2$ MHz. Because the line maximum at room temperature corresponding to $p=0$ is at $\omega_0/2\pi=12.1$ MHz a value $\omega_1=2.9$ MHz results. With this

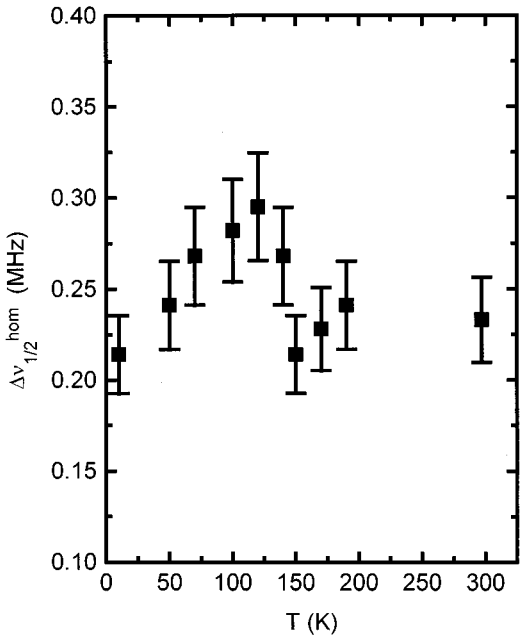

FIG. 7. Temperature dependence of the homogeneous part of the ENDOR line width $\Delta\nu_{1/2}^{\mathrm{hom}}$ of proton $H13$ extracted from the 2D HYSCORE spectra for which examples are presented in Fig. 6 in the manner as explained in the text.

experimental normalization procedure the peak position of the ENDOR line at 90 K corresponds to $p=0.7$ in good agreement to the Tikhonov regularization results.

Relaxation time measurements

Additionally, measurements of the spin-lattice relaxation time T_1 of the PO_3^{2-} center in $BP_{0.15}BPI_{0.85}$ single crystals were performed in the temperature range from 4 K to room temperature. The results are presented in Fig. 10. The temperature dependence of the spin-lattice relaxation rate T_1^{-1} is

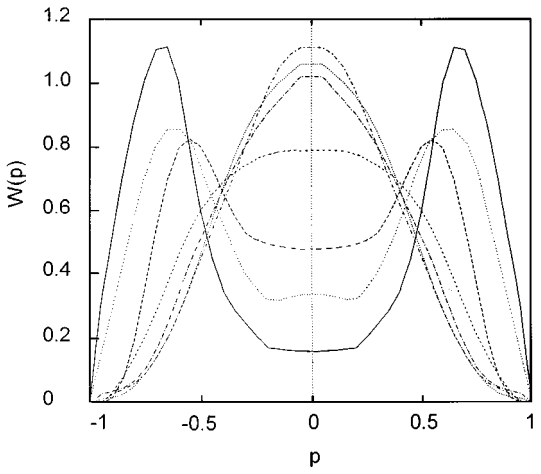

FIG. 8. Local order parameter distribution function $W(p)$ of proton $H13$ attached to the PO_3^{2-} center in $BP_{0.15}BPI_{0.85}$ obtained from the ENDOR spectra shown in Fig. 4 by means of the Tikhonov regularization method for the following temperatures: 290 (highest value at $p=0$), 250, 210, 170, 130, 120, and 90 K (lowest value at $p=0$).

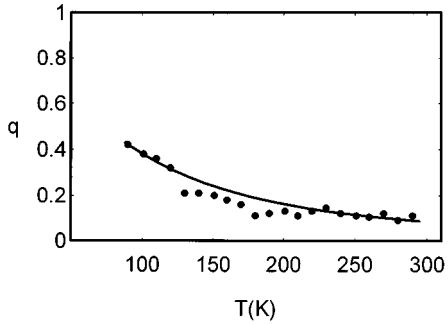

FIG. 9. Temperature dependence of the Edwards-Anderson order parameter q for proton $H13$ attached to the PO_3^{2-} center in $BP_{0.15}BPI_{0.85}$: (a) points—experimental q values obtained as the second moment of the experimental order parameter distribution functions shown in Fig. 8, and (b) drawn line—simulated $q(T)$ dependence calculated with the 3D and 1D RBRF model as well with zero-mean J_0 using the parameter sets as given in the text.

very similar to that of the $BP_{0.40}BPI_{0.60}$ mixed crystal already published.[37] Without going into the details of explanation of the relaxation processes induced by optical Raman processes and phonon assisted tunneling as explained in our former paper,[37] we want to focus our attention on the temperature anomaly observed at about 150 K in $BP_{0.15}BPI_{0.85}$. A similar anomaly was also seen in $BP_{0.40}BPI_{0.60}$ and in pure BPI (Ref. 37) but at temperatures of about 140 and 200 K, respectively. We related this anomaly to an anomaly of the damping of the internal optical phosphite mode at 1.6×10^{13} Hz. This mode seems to be critically damped at the ferroelectric transition in BPI which causes the T_1 anomaly. Because we probe the mixed crystals with the same paramagnetic PO_3^{2-} center, we may conclude that also in $BP_{0.15}BPI_{0.85}$ this mode experi-

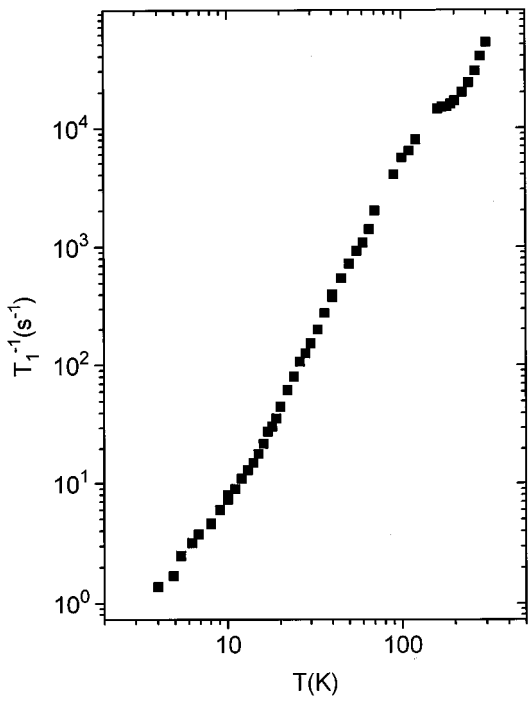

FIG. 10. Temperature dependence of the spin-lattice relaxation rate T_1^{-1} of the PO_3^{2-} center in γ-irradiated $BP_{0.15}BPI_{0.85}$ with magnetic field $\underline{B}\|b$.

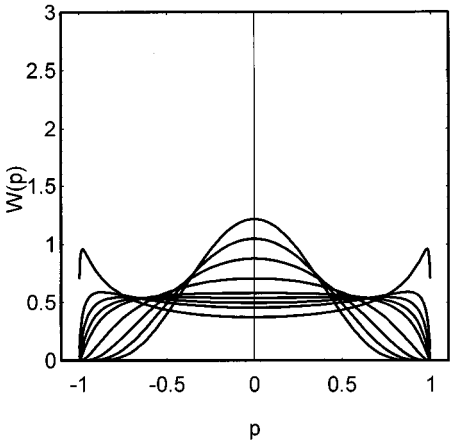

FIG. 11. Simulation of the local order parameter distribution functions $W(p)$ using the 3D RBRF model with zero-mean $\tilde{J}_0=0$, $\tilde{J}/k_B=30$ K, and $\tilde{\Delta}=10$ for the following temperatures: 290 (highest value at $p=0$), 250, 210, 170, 140, 130, 120, and 90 K (lowest value at $p=0$).

ences a critical damping due to a structural transition at about 150 K until now unknown.

V. COMPARISON OF THE ENDOR RESULTS WITH THE THEORETICAL MODELS

3D RBRF Ising Model

To get an estimate of the random field variance we did simulations of the experimental temperature dependence of the Edwards-Anderson order parameter q with Eq. (9) taking $\tilde{J}/k_B=T_G=30$ K from the dielectric measurements,[21] zero mean bond interaction $\tilde{J}=0$, and $\tilde{\Delta}=10$ corresponding to $T_f\approx(95\pm5)$ K. The result is shown in Fig. 9. The large random fields in $BP_{0.15}BPI_{0.85}$ generated by substitutional disorder induce the random local polarization of the protons in the O-H···O bonds far above T_G as observed in the ^{1}H ENDOR spectra.

The change in the shape of the distribution function $W(p)$ from a single-peak Gaussian distribution to a double-peak structure far above T_G is at the first view typical for proton and deuteron glasses when local random fields are dominant.[28,29] A simulation of $W(p)$ with Eq. (13) for different temperatures using the parameters $\tilde{J}/k_B=30$ K, $\tilde{\Delta}=10$ and a zero mean bond interaction $J_0=0$ is shown in Fig. 11. However, the simulated distribution functions $W(p)$ do not very well agree with the $W(p)$ distributions obtained by the ^{1}H ENDOR line shape analysis (Fig. 8). Especially, the gradual change from the flattened structure into the double peak shape cannot be simulated with the above parameters. We also calculated $W(p)$ with Eq. (13) using $J_0=0$ and other parameters sets of J and $\tilde{\Delta}=0$ but no set of data gave satisfactory agreement with the experimental distributions.

1D RBRF Ising Model

From this disagreement one could conclude that the 3D RBRF Ising model of proton glasses with infinite-range interactions is not adequate for the hydrogen bonded system in $BP_{0.15}BPI_{0.85}$. Because the hydrogen bonds link the HPO_3 and or PO_4 groups to quasi-one-dimensional chains one could suspect that the interactions between the quasispins within the chains are dominating in comparison to those between quasispins in different chains[7,8] and therefore, $BP_{0.15}BPI_{0.85}$ might be described more adequately by a quasi-one-dimensional Ising model as described in Sec. III.

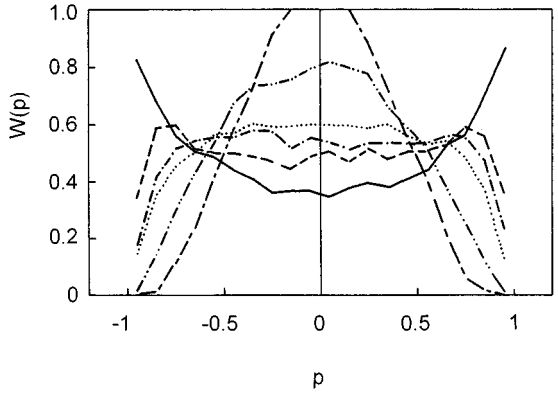

FIG. 12. Simulation of the local order parameter distribution functions $W(p)$ using the 1D RBRF model with zero-mean $\tilde{J}_0=0$, $\tilde{J}/k_B=K/k_B=70$ K, and $\tilde{\Delta}=0.8$ for the following temperatures: 200 (highest value at $p=0$), 160, 130, 120, 110, and 90 K (lowest value at $p=0$).

The numerical calculation of q with the parameter sets $J=K=30$ K, $\tilde{\Delta}=8$ ($T_f=85$ K) and $J=K=70$ K, $\tilde{\Delta}=0.8$ ($T_f=63$ K), respectively, for a chain with $N=10^3$ quasispins leads to a temperature dependence of q not distinguishable from that calculated with the 3D RBRF model in the last subsection. The $W(p)$ distribution was estimated with the second parameter set for $N=10^4$ by calculating $\langle\sigma_i\rangle$ according to Eq. (27) in Ref. 36 and then counting the number of spins the individual order parameter of which are within each of 20 intervals between $+1$ and -1. The result is shown in Fig. 12. The qualitative behavior of $W(p)$ in the 1D model is similar to that of the 3D model but can also only poorly explain the experimental behavior shown in Fig. 8. Therefore, there is no indication for a more adequate description of the proton order in $BP_{0.15}BPI_{0.85}$ by the 1D model.

3D RBRF Ising Model with nonzero mean J_0

The deviations of the experimentally determined $W(p)$ distribution from those calculated with the 3D and 1D RBRF model with zero mean J_0 become obvious for temperatures below 150 K. The observed behavior seems to be indicative for a smeared-out phase transition to a long-ranged ordered phase. Therefore, we tried to simulate the $W(p)$ distribution with the 3D RBRF Ising model with non-zero-mean J_0. In order to obtain a $W(p)$ behavior similar to the experimental one, the variance of the random fields at temperature below $T_0=J_0/k_B$ must be taken as a temperature-dependent simulation parameter. The optimized simulations adapted to experimental $W(p)$ and q_{EA} values are shown in Fig. 13. Above $J_0/k_B=160$ K the variance parameters $\tilde{\Delta}=7$ and $\tilde{J}/k_B=30$ K give reasonable results. Below 160 K one has to reduce $\tilde{\Delta}$ in order to be able to describe the experimental $W(p)$ curves with the model. With $J_0/k_B=160$ K, $\tilde{J}/k_B=30$ K, and $\Delta=2$ one obtains a non-zero-mean order parameter $\tilde{p}\neq0$ below $T_C=144$ K. This results in peaks of $W(p)$ at

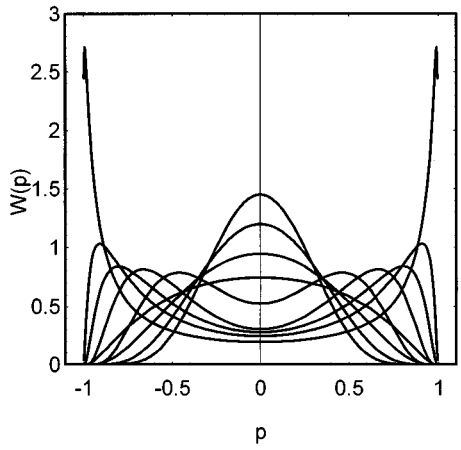

FIG. 13. Simulation of the local order parameter distribution functions $W(p)$ by means of the 3D RBRF model with non-zero-mean $\tilde{J}_0/k_B=160$, $\tilde{J}/k_B=30$ K, using a constant random field variance parameter $\tilde{\Delta}=7$ for the temperatures 290 (highest value at $p=0$), 250, 210, 170 K, but temperature dependent parameters $\tilde{\Delta}=2$ for 140, $\tilde{\Delta}=2.5$ for 130, $\tilde{\Delta}=3.5$ for 120, $\tilde{\Delta}=4.5$ for 110, and $\tilde{\Delta}=6.5$ for 90 K (lowest value at $p=0$).

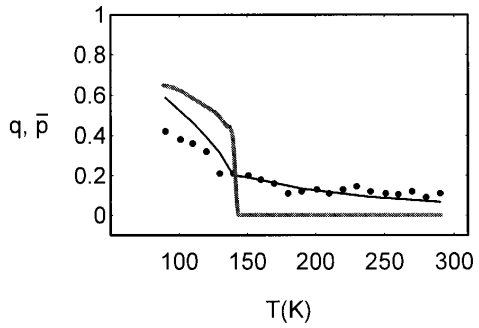

FIG. 14. Simulated temperature dependence of the Edwards-Anderson order parameter q (thin line) and the long-range order parameter $\overline{p}$ (thick line) using the 3D RBRF model with non-zero-mean $\tilde{J}_0/k_B=160$ K and the same parameter set as given in Fig. 13. The points are again the experimental q values obtained as the second moments of the experimental $W(p)$ distributions shown in Fig. 8.

$p\geqslant 0.5$ as experimentally observed, but only when the random field variance was drastically reduced below the transition temperature to $\tilde{\Delta}=2.0$, 2.5, 3.5, and 4.5 at 140, 130, 120, and 110 K, respectively. The calculated q and $\overline{p}$ values are shown in Fig. 14. The used parameter sets are a compromise of best agreement between the simulated and the experimental results of $W(p)$ for the obtained temperature-dependent values of the Edwards-Anderson order parameter q.

VI. DISCUSSION AND CONCLUSIONS

The ENDOR investigations of the $BP_{0.15}BPI_{0.85}$ mixed crystal give a direct experimental evidence for a temperature dependent local order of the protons $H13$ and $H15$ in the hydrogen bonds linking the phosphite and phosphate groups to chains along the monoclinic b axis. The proton $H12$ in the hydrogen bond linking the phosphite group with the carboxyl group of the betaine molecule is clearly not involved in the ordering process. The comparison of the experimentally determined temperature dependence of the Edwards-Anderson order parameter of the protons $H13$ and $H15$ in the hydrogen bridges with those calculated from the 3D and 1D RFRB model indicates that $BP_{0.15}BPI_{0.85}$ behaves as a proton glass with strong random fields. The unusually large random field variance parameter $\tilde{\Delta}$ which we had to use in order to simulate the experimental results shows us that the substitution of an HPO_3 group by a PO_4 group leads to strong distortions of the adjacent hydrogen bonds linking the substituted group with the others. This is also directly seen from not yet published ^{1}H ENDOR and HYSCORE spectra of the phosphate-rich mixed crystal $BP_{0.95}BPI_{0.05}$ where the paramagnetic PO_3^{2-} center probes a substitution site which is with high probability surrounded by phosphate groups. The ENDOR lines of the adjacent protons $H13$ and $H15$ appear at positions which show that already at room temperature both protons are off-center. It comes out that in the PO_4-$H13$-PO_3-$H15$-PO_4 cluster the proton $H13$ is shifted towards the PO_4 group whereas proton $H15$ has a position closer to the PO_3 group. That means that in this cluster the local polarization of both protons is such as that created by a local bias field at the substitutional PO_3 site.

It is interesting to note that the experimentally determined order parameter distribution function $W(p)$ of the protons in $BP_{0.15}BPI_{0.85}$ gives much deeper insight into the proton order of the hydrogen bridges in the chains than the Edwards-Anderson order parameter expressed as its integral. Already an inspection of Fig. 4 reveals remarkable deviations of the modeled q values from the experimental one. A comparison of Fig. 8 with Fig. 11 and Fig. 12 shows very evidently the lack of agreement of the experiment with the 1D and 3D RBRF model in $W(p)$. The modeled $W(p)$ distribution functions show only rough similarity with those experimentally obtained. Whereas the agreement at higher temperatures is acceptable, distinct deviations appear below 170 K. The experimentally obtained $W(p)$ distribution functions show at lower temperatures pronounced maxima at local order parameter values $|p|<1$ which are shifted to larger $|p|$ with lowering the temperature. This behavior cannot be simulated within the framework of the 1D or 3D RBRF model without long-range order. There are no indications for a more adequate description of the proton glass behavior in $BP_{0.15}BPI_{0.85}$ when the 1D model is used. This was also the result of dielectric investigations.[23] Probably, the strong random fields cover the weaker dimensional dependent random bond interactions.

A better agreement is achieved when a long-range proton order is introduced in the 3D RBRF model using a non-zero-mean $\tilde{J}_0$ of the bond interactions. Now, the pronounced maxima in the order parameter distribution function as well as their temperature-dependent position can be simulated qualitatively. Also the processed temperature dependence of the Edwards-Anderson order parameter shows better agreement with the experimental values insofar as for temperatures above 140 K the simulation succeeds rather well and the rapid increase to lower temperatures can be described at least qualitatively. The non-zero-mean value $\tilde{J}_0/k_B=160$ K means that a long-range ferroelectric or antiferroelectric proton order takes place in the hydrogen bond system of the chains below the transition temperature $T_C=145$ K which

results from $\tilde{J}_0$ and the Edwards-Anderson order parameter $q \approx 0.2$ in this temperature region. This transition temperature is far above the freezing temperature $T_f = 95$ K and the glass transition temperature $T_G = 30$ K. However, one must also remember that the simulation of both the temperature dependent order parameter distribution function $W(p)$ and the Edwards-Anderson order parameter only succeeds when the random field variance is not temperature independent but strongly reduced at and below the phase transition temperature T_C. As discussed above, the random fields in the mixed crystal are related to distortions in the hydrogen bonds adjacent to the substitutional PO_4 group in such a manner that their proton order is strongly biased. A reduced random field variance at T_C could mean that the local proton polarizations are rearranged within one growing domain in such a way that the polarization direction of most of the biased substitutional sites coincides with that in the domain. With lower temperature the domains grow up, and more and more substitutional sites conflict with their surrounding domains leading to increased local random fields.

An additional confirmation for a phase transition in that temperature range comes from the results of the electron spin-lattice relaxation time measurements performed at the PO_3^{2-} center in $BP_{0.15}BPI_{0.85}$ and shown in Fig. 10. The observed temperature anomaly of the spin-lattice relaxation rate T_1^{-1} close to the above transition temperature T_C is an indication for a structural phase transition. As already mentioned in Sec. IV, also in the $BP_{0.40}BPI_{0.60}$ mixed crystal a similar T_1 anomaly was observed at a comparable temperature.[37] This can indicate that the phase with a strongly distorted long-range proton order in the hydrogen bonds of the phosphate/phosphite chains does not only exist in the $BP_{0.15}BPI_{0.85}$ compound but in a extended composition range of the phase diagram.

In this context, it is interesting to point out that Ebert *et al.*[38] reported on pressure-dependent dielectric measurements on pure betaine phosphite. Two additional transitions were found under a hydrostatic pressure of 350 MPa at $T_{d1} \approx 150$ K and $T_{d2} = 85$ K which collapse into one at $T_d = 142$ K under zero pressure as already known from former measurements.[39] From that they concluded on three different regions in the formerly called ferroelectric phase of betaine phosphite: (a) a ferroelectric phase up to T_{d1}, (b) a pseudoferroelectric phase between T_{d1} and T_{d2} where the ferroelectric order is continuously broken due to a freezing process with frozen-in or frustrated regions, and (c) a clusterlike phase below T_{d2} with fixed domain structure. Also in betaine phosphate a ferroelectric phase was reported[5] in a small temperature interval above the transition temperature into the antiferroelectric phase at 81 K. One could speculate that it is such an intermediate phase which we see in the proton order of the $BP_{0.15}BPI_{0.85}$ mixed crystal.

At the end there is still one very important point to be discussed. It concerns the obvious disagreement of the experimental and simulated behavior of Edwards-Anderson order parameter and order parameter distribution function at the lowest temperatures. The simulations at 90 K lead always to sharp maxima of $W(p)$ close to $p = \pm 1$ whereas the experimentally obtained distribution function $W(p)$ shows its maxima at $p = \pm 0.7$. This deviation of the position of the extrema is far outside of the experimental error as already demonstrated in Sec. IV. It shows that the local proton polarization is limited to values distinctly below $|p| = 1$ at low temperatures in $BP_{0.15}BPI_{0.85}$. In relation with this interesting effect we must remember that we did ignore proton tunneling till now. The models which we used for simulations have been worked out for deuteron glasses where tunneling is not of importance. Dattagupta *et al.*[31] published a stochastic theory that considers the influence of tunneling on the NMR line shape in proton glasses. The authors showed that the local proton polarization is reduced due to tunneling by a factor r which is the ratio between the local fields seen by the proton without and with the tunneling contribution,

$$r(z) = h(z)/h_0(z)$$

with $h_0 = \sqrt{\Omega^2 + h(z)^2}$, where Ω is the tunneling energy. Estimations lead to a value for the tunneling energy of the order in $\Omega/k_B = 200$ K when $r = 0.7$ shall be obtained. On the other hand, if one tries to explain the shift of the ferroelectric transition temperature due to deuteration in betaine phosphite within the tunneling model[40] a tunneling energy of the same order of magnitude, $\Omega/k_B = 440$ K, results. Therefore, we suggest that proton tunneling in the hydrogen bonds of the phosphite/phosphate chains is of relevant importance in betaine phosphate/betaine phosphite proton glasses.

ACKNOWLEDGMENTS

This work was supported by the Deutsche Forschungsgemeinschaft and by the Humboldt-Stiftung.

[1] J. Albers, A. Klöpperpieper, H. J. Rother, and K. Ehses, Phys. Status Solidi A **74**, 533 (1982).

[2] J. Albers, A. Klöpperpieper, H. E. Müser, and H. J. Rother, Ferroelectrics **54**, 45 (1984).

[3] J. Albers, A. Klöpperpieper, H. J. Rother, and S. Haussühl, Ferroelectrics **81**, 27 (1988).

[4] D. Schaack, Ferroelectrics **104**, 147 (1990).

[5] M. Lopes dos Santos, J. M. Kiat, A. Almeida, M. R. Chaves, A. Klöpperpieper, and J. Albers, Phys. Status Solidi B **189**, 371 (1995).

[6] W. Schildkamp and J. Spilker, Z. Kristallogr. **168**, 159 (1984).

[7] I. Fehst, M. Paasch, S. L. Hutton, M. Braune, R. Böhmer, A. Loidl, M. Dörffel, Th. Narz, S. Haussühl, and G. J. McIntyre, Ferroelectrics **138**, 1 (1993).

[8] G. Fischer, H. J. Brückner, A. Klöpperpieper, H. G. Unruh, and A. Levstik, Z. Phys. B **79**, 391 (1990).

[9] H. J. Brückner, H. G. Unruh, G. Fischer, and L. Genzel, Z. Phys. B **71**, 225 (1988).

[10] H. Bauch, J. Banys, R. Böttcher, A. Pöppl, G. Völkel, and C. Klimm, Ferroelectrics **163**, 59 (1995).

[11] H. Bauch, R. Böttcher, and G. Völkel, Phys. Status Solidi B **178**, K39 (1993).

[12] H. Bauch, R. Böttcher, and G. Völkel, Phys. Status Solidi B **179**, K41 (1993).

[13] H. Bauch, R. Böttcher, and G. Völkel, Phys. Status Solidi B **179**, K93 (1993).
[14] G. Völkel, H. Bauch, R. Böttcher, A. Pöppl, J. Simon, and A. Klöpperpieper, Mol. Phys. Rep. **5**, 292 1994.
[15] A. Pöppl, G. Völkel, H. Metz, and A. Klöpperpieper, Phys. Status Solidi B **184**, 471 (1994).
[16] R. Sobiestanskas, J. Grigas, Z. Czapla, and S. Dacko, Phys. Status Solidi A **136**, 223 (1993).
[17] e.g., F. Jona and G. Shirane, *Ferroelectric Crystals* (Pergamon, Oxford, 1962).
[18] S. L. Hutton, I. Fehst, R. Böhmer, M. Braune, B. Mertz, P. Lunkenheimer, and A. Loidl, Phys. Rev. Lett. **66**, 1990 (1991).
[19] M. L. Santos, J. C. Azevedo, A. Almeida, M. R. Chaves, A. R. Pires, H. E. Müser, and A. Klöpperpieper, Ferroelectrics **108**, 1969 (1990).
[20] M. L. Santos, M. R. Chaves, A. Almeida, A. Klöpperpieper, H. E. Müser, and J. Albers, Ferroelectr. Lett. **15**, 17 (1993).
[21] J. Banys, C. Klimm, G. Völkel, H. Bauch, and A. Klöpperpieper, Phys. Rev. B **50**, 16 751 (1994).
[22] A. Loidl and R. Böhmer, in *Glass Transitions and Relaxational Phenomena in Orientational Glasses and Supercooled Crystals*, edited by A. Blumen and R. Richert, Disorder Effects on Relaxational Processes (Springer, Heidelberg, in press).
[23] H. Ries, R. Böhmer, I. Fehst, and A. Loidl (unpublished).
[24] J. Menberger, H. Ries, and A. Loidl (unpublished).
[25] S. F. Edwards and P. W. Anderson, J. Phys. F **5**, 965 (1975).
[26] D. Sherrington and S. Kirkpatrick, Phys. Rev. Lett. **35**, 1792 (1975).
[27] R. Blinc, Z. Naturforsch. **45a**, 313 (1989).
[28] R. Pirc, B. Tadic, R. Blinc, and R. Kind, Phys. Rev. B **43**, 2501 (1991).
[29] R. Kind, R. Blinc, J. Dolinsek, N. Korner, B. Zalar, P. Cevc, N. S. Dalal, and J. DeLooze, Phys. Rev. B **43**, 2511 (1991).
[30] H. Schäfer and H. Bauch, Phys. Lett. A **199**, 93 (1995).
[31] S. Dattagupta, B. Tadic, R. Pirc, and R. Blinc, Phys. Rev. B **44**, 4387 (1991).
[32] S. Dattagupta, B. Tadic, R. Pirc, and R. Blinc, Phys. Rev. B **47**, 8801 (1993).
[33] P. Höfer, A. Grupp, H. Nebenführ, and M. Mehring, Chem. Phys. Lett. **132**, 279 (1986).
[34] A. Pöppl, R. Böttcher, and G. Völkel, J. Magn. Reson. **A120**, 214 (1996).
[35] M. Oresic and R. Pirc, Phys. Rev. B **47**, 2655 (1993).
[36] P. Höfer, J. Magn. Res. **A111**, 77 (1994).
[37] A. Pöppl, G. Völkel, J. Hoentsch, S. Orlinski, and A. Klöpperpieper, Chem. Phys. Lett. **224**, 233 (1994).
[38] H. Ebert, S. Lanceros-Mendez, G. Schaack, and A. Klöpperpieper, J. Phys. Condens. Matter **7**, 9305 (1995).
[39] H. Bauch, J. Banys, R. Böttcher, C. Klimm, A. Klöpperpieper, and G. Völkel, Phys. Status Solidi B **187**, K81 (1995).
[40] R. Blinc and B. Zeks, *Soft Modes in Ferroelectrics and Antiferroelectrics* (North-Holland, Amsterdam, 1974).